Proc. Indian Acad. Sci. (Earth Planet. Sci.), Vol. 89, Number 3, November 1980, pp. 413–430.

Geoelectrical response of a water bearing sandstone-shale sequence and the estimation of sandstone-shale ratios

SRI NIWAS, A K AWASTHI and S MANTRI*
Department of Earth Sciences, University of Roorkee, Roorkee 247 672, India
*Rajasthan Ground Water Board, Jodhpur, Rajasthan, India

MS received 6 May 1980

Abstract. An attempt has been made to use the geoelectrical response of a water bearing sandstone-shale sequence to estimate the sandstone-shale ratio. In all, 168 sandstone-shale sequence models were generated using Monte-Carlo simulation technique. The resistivity transform and its autocorrelation function of all the models were calculated. The amplitude, phase, power and log spectra were also extracted. The power spectrum appears to hold promise in estimating the sandstone-shale ratio of these models because the power amplitude P_2 shows a high negative correlation with sandstone shale ratio values.

Keywords. Monte-Carlo simulation; power spectrum; geoelectrical response; sandstone; sandstone-shale ratio; resistivity transform; autocorrelation; spectral analysis.

1. Introduction

The need for developing methodology for assessment of groundwater resources is universal and earth scientists are continuously engaged in developing more and more dependable techniques for assessing these hidden resources. The geological structures, lithological characters and stratigraphy provide the framework in which ground water recharge, storage and discharge take place. Amongst the sedimentary sections of elastic rocks, the sandstone-shale sequences are quite frequently observed in nature. The petrophysical parameters make sandstone a good aquifer. In such sequences the higher the percentage of sandstone, the higher the amount of water is expected. An accurate determination of subsurface sandstone-shale sequence in an area by remote sensing methods should, therefore, provide a good insight into the ground water potential of that area.

Many new approaches for mapping subsurface stratigraphic sequences using seismic data have been proposed recently. Seismic interval velocity has become the most significant parameter for identifying lithologies (Smith 1969; Taner and Kochler, 1969; Taner *et al* 1970; Gardner *et al* 1974). Savit and Matekar (1971) proposed the use of seismic energy attenuation as a guide to subsurface

lithology. Mathieu and Rice (1969) attempted a discriminatory analysis of a linear combination of more than one observed parameter of the seismic trace to study the variation in stratigraphic conditions. Avasthi and Verma (1973) proposed a multiple parameter approach to the problem of inferring stratigraphy from seismic data. Khattri and Gir (1975, 1976) used a deterministic approach for extracting the sand-shale ratio from information contained within the seismogram. A more general statistical approach has been suggested by Khattri *et al* (1979). Their procedure relied upon Monte-Carlo simulation of models. Discriminant characteristics were selected from processed seismic data, thus increasing the degree of success.

All these studies were carried out to locate stratigraphic traps for oil using seismic signals. The present study attempts to explore the possibilities of utilising electrical resistivity signals at the surface in deciphering the sandstone-shale sequences and their groundwater potentialities. Sri Niwas *et al* (1978) attempted to evaluate certain geophysical parameters for determining sand-shale ratio in sedimentary section from the resistivity transform function (Koefoed 1970) and its processed forms. The resistivity transform function can quickly and efficiently be extracted from the apparent resistivity data using Ghosh (1971) filter. The present study was taken up to further improve the technique adopted by Sri Niwas *et al* (1978). A suitable window for avoiding undesirable Gibb's phenomenon has been applied.

In all, 168 sandstone-shale models with ratio values ranging from 0·15 to 0·95 were simulated using Monte-Carlo technique. The resistivity transform function and its processed forms, autocorrelation function, amplitude, phase, power and log spectra have been critically evaluated for all the models. The parameters considered for preliminary statistical analysis have been empirically chosen from the processed forms of the resistivity transform function. The power spectrum holds promise towards the evaluation of a geological section (sandstone-shale alternations) in terms of sandstone-shale ratio.

2. Theoretical consideration

2.1. *Generation of models*

The multiplicative congruential method (Harbough and Carter 1970) yields a sequence of numbers which are uniformally distributed. In nature, however, the frequency distributions of most variables are not uniform. Many geological variables are log normally distributed. Assuming the distribution of thickness of the sedimentary units to follow log-normal distribution, the sandstone shale alternations can be generated using Monte-Carlo method. The scheme for generating log normally distributed random numbers is given by

$$X' = \exp\left[\mu_{y'} + \sigma_{y'}\left(\frac{\sum_{i=1}^{K} r_i - 6}{(K/12)^{1/2}}\right)\right], \qquad (1)$$

where $y' = \log_e X'$, r_i is the ith element of sequence of random numbers drawn from a uniform distribution in the range 0·0 to 1·0, $\mu_{y'}$ is the mean of y', $\sigma_{y'}$ is the standard deviation of y' and K is the number of values of r_i to be used.

If $K = 12$, a normal distribution with tails truncated at six standard deviation is produced. For most applications this is adequate ; if tail probabilities are critical beyond these points, K must be increased accordingly. With $K = 12$ equation (1) gets reduced to

$$X' = \exp\ [\mu_{y'} + \sigma_{y'} (\sum_{i=1}^{12} r_i - 6)]. \tag{2}$$

2.2. *Constraints on the model*

Groundwater is known to occur in porous and permeable rocks. The exploration and evaluation of groundwater of an unconfined aquifer is not much of a problem. The real problem comes when artisan conditions are dealt with. In the present study, therefore, sandstone-shale sedimentary sequences with confined water conditions have been taken up. Water has been assumed to be confined within the porous and permeable sandstone sandwitched between impervious shale.

In order to make mathematical analysis easier certain assumptions have been made. It is assumed that the subsurface is a layered medium. The layers are homogeneous, isotropic, of infinite lateral extent and nearly horizontal. The sandstone-shale sequences have been assumed to be capped by a surface layer of massive limestone. It is also assumed that the bottom layer is of infinite thickness.

There are some constraints on the models due to geohydrological considerations. The thickness of the topmost limestone layer has been fixed at 5 m. The thickness of other layers have been restricted to various ranges, the minimum value of which is 1 m. A sandstone aquifer of thickness less than 1 m is in actual practice of no economic value. At the same time a shale layer of thickness less than 1 m may not act as an impervious layer. The model generation technique ensures that there are at least two sandstone layers in each model. Another constraint is on the total thickness of the geohydrological section which was fixed at 300 m ± 3 m.

2.3. *Resistivity transform*

The potential due to a point current source at the surface of layered earth can be written as (Stefanesco and Schlumbarger 1930)

$$V = \frac{I\rho_1}{2\pi}\left[\frac{1}{r} + 2\int_0^\infty K(\lambda)\, J_0(\lambda r)\, d\lambda\right], \tag{3}$$

where notations have their well-established meaning. Equation (3) can also be written as

$$V = \frac{I}{2\pi}\int_0^\infty T(\lambda)\, J_0(\lambda r)\, d\lambda, \tag{4}$$

where $T(\lambda) = \rho_1 [1 + 2K(\lambda)]$ and is known as resistivity transform. Utilising expression for apparent resistivity for Schlumberger configuration

$$\rho_{as} = -\frac{2\pi}{I} s^2 \left(\frac{\partial V}{\partial r}\right)_{r=s}$$

equation (4) can be written after applying Hankel transform as,

$$T(\lambda) = \int_0^\infty \rho_{as}(s)\, J_1(\lambda s)\, \frac{ds}{s}\,. \tag{5}$$

Ghosh (1971) presented equation (5) as convolution integral after defining new set of variables, $x = \ln s$ and $y = \ln(1/\lambda)$ as

$$T(e^{-y}) = \int_{-\infty}^{\infty} \rho_{as}(e^{x})\, J_1(e^{-(y-x)})\, dx. \tag{6}$$

Equation (6) helps us to extract resistivity transform from field measurements (Ghosh 1971).

The initial step in the theoretical evaluation of $T(\lambda)$ would be the determination of the kernel function $K(\lambda)$. The kernel function is quotient in which both the numerator and the denominator are polynomial in $e^{-2\lambda}$. Flathe (1955) introduced kernel function for n-layer earth as

$$K(v) = P_n(v)/Q_n(v), \tag{7}$$

where $e^{-2\lambda} = e^{-2/u} = v$, $1/\lambda = u$, and $Q_n(v) = H_n(v) - P_n(v)$. The index n gives the number of layers.

Flathe (1955) gave the recurrence relation for the polynomials $P_n(v)$ and $H_n(v)$ over the multilayered section as

$$\left.\begin{aligned} P_n(v) &= P_{n-1}(v) + H_{n-1}(v^{-1})\, k_{n-1} v^{h_{n-1}} \\ H_n(v) &= H_{n-1}(v) + P_{n-1}(v^{-1})\, k_{n-1} v^{h_{n-1}} \end{aligned}\right\}. \tag{8}$$

The k_{n-1} in the above relation is given by

$$k_{n-1} = \frac{\rho_n - \rho_{n-1}}{\rho_n + \rho_{n-1}}\,.$$

ρ_n and ρ_{n-1} represents the resistivities of the nth layer and $(n-1)$th layer respectively and h_{n-1} is the depth to $(n-1)$th interface. Thus if $P_n(v)$ and $H_n(v)$ are known for a particular value of $n = m$, then these polynomials can be calculated for $n = m + 1$ using equation (8) provided that the sequences $\rho_1, \rho_2 \ldots, \rho_{m+1}$ are known.

Starting from a small value of $1/\lambda$ and giving successive increment equation (7) can be effectively used for numerical calculation of the kernel function. Once the kernel function is obtained for a particular value of $1/\lambda$, a simple calculation using $T(u) = \rho_1[1 + 2K(u)]$ will yield the corresponding resistivity transform function.

3. Procedure

3.1. *Generation of models*

In order to have sufficient random models, 168 sandstone shale models have been generated using Monte-Carlo simulation technique. The sandstone-shale ratio

varies from 0·15 to 0·95. This ratio range was divided into four small subgroups due to unavoidable clustering of points within a small range (see table 1). In each subgroup 42 models were generated using the method given by Harbaugh and Carter (1970) with some modification taking into account the constraints imposed on the models. With the assumed lognormal distribution of thicknesses, equation (2) has been used to generate these models. The mean and standard deviation of thickness of sandstone and shale for various ratio ranges are listed in table 2. With the restriction of a minimum of two sandstone layers in each model, the maximum thickness of sandstone and shale layers for various ratio ranges is given in table 2.

The resistivity of water-bearing sandstone in all models has been taken to be 40 Ωm and for shale 10 Ωm. The resistivity of the massive overlying hard rock was assumed to be 80 Ωm. These values of resistivities are comparable with the resistivities obtained in actual sandstone-shale sections with fresh water. The resistivity of the basement is assumed to be very large, approaching infinity.

3.2. *Computation of resistivity transform*

Next step after the generation of sandstone-shale models is the calculation of the resistivity transform for each of the 168 models. The scheme for calculation is based on recurrence relation of Flathe (1955). For computational purposes, the

Table 1. Range of variation kept for generation of sandstone and shale layers.

Group No.	Sand-shale ratio range	Minimum sand or shale thickness m	Maximum sand thickness of one layer m	Maximum shale thickness of one layer m
1	0·15–0·35	1·0	30·0	270·0
2	0·35–0·55	1·0	60·0	240·0
3	0·55–0·75	1·0	90·0	210·0
4	0·75–0·95	1·0	120·0	180·0

Table 2. Specified means and standard deviation for generation of log normal thickness.

Group No.	Sand-shale ratio range	For sand specified		For Shale specified	
		Mean	Std. deviation	Mean	Std. deviation
1	0·15–0·35	1·7006	0·2834	2·7993	0·4665
2	0·35–0·55	2·0472	0·3412	2·7404	0·4567
3	0·55–0·75	2·2499	0·3750	2·6736	0·4456
4	0·75–0·95	2·3938	0·3990	2·5965	0·4328

resistivity transform has to be specified by a discrete series in which all terms are sampled at a uniform Nyquist interval so that the transform can be exactly reproduced from its discretised values. The Nyquist rule of largest permissible sampling interval is $\triangle x = 1/2fc$, fc is the cut-off frequency and $\triangle x$ is the sample interval. In the present analysis $\triangle x$ has been fixed at ln (10)/10 = 0·230.

3.3. *Computation of autocorrelation*

To study the average character or the self-comparison of the resistivity transform in space domain, the autocorrelation function of the resistivity transform for each model has been computed. If the sampled values of signal denoted by $T(u)$ are at uniform interval τ, then the autocorrelation function of $T(u)$ is given by

$$C_{11}(\tau) = \frac{1}{N-\tau} \sum_{u=1}^{N-\tau} T(u)\, T(u+\tau), \tag{9}$$

where $\tau = 0, 1, 2, \ldots m$ and the given space series is $T(1), T(2) \ldots T(N)$. The maximum value of autocorrelation function is at zero lag. For resistivity transform both m and N were fixed at 40.

3.4. *Spectral analysis*

The amplitude, phase, power and log spectrum of the resistivity transform were calculated with the help of Fourier transform after applying Tukey window.

The whole procedure adopted in the present analysis is presented in figure 1 in the form of block diagram.

4. Analysis and discussion of results

Based on the procedure discussed above, the sandstone-shale models were generated. A few of these representative models for each of the sandstone-shale ratio groups are shown in figure 2 depicting the lithological variations. Figure 2 shows variability in the thickness of each layer not only within sections but also amongst various models. The number of layers in these models varies from 19 to 27.

4.1. *Resistivity transform*

The resistivity transform for the various models were plotted on bilog graph papers of modulus 62·5 mm, a few of which are shown in figures 3 and 4. The nature of the resistivity transform curve for all the models is essentially of descending type. No major discriminant for sandstone-shale value is discernible by superposition of these curves.

4.2. *Autocorrelation function*

The autocorrelation function was obtained for entire data length and are graphically presented for some selected models in figure 5. The nature of the autocorrelation function for the zero lag is also of descending type. Superposition

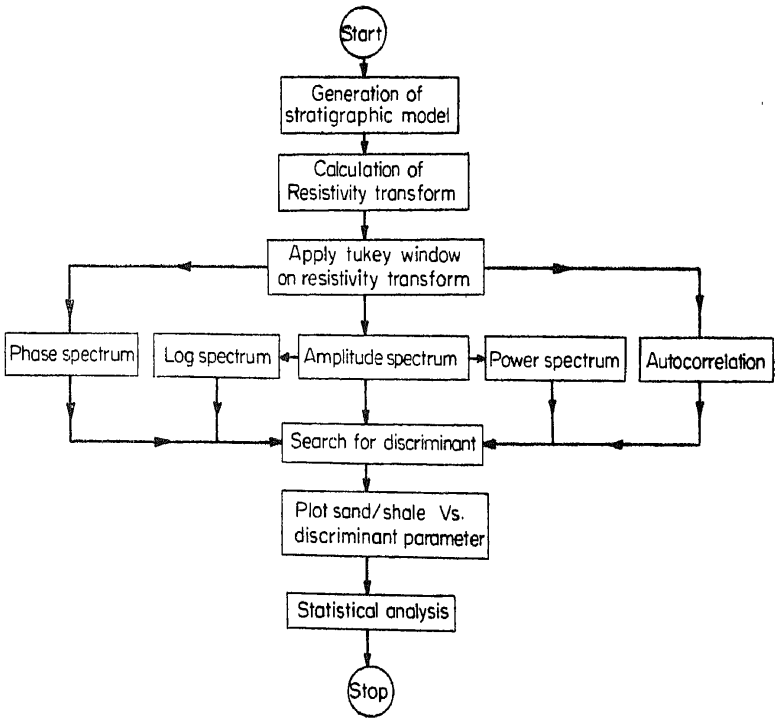

Figure 1. Block diagram of the procedure adopted in the present analysis.

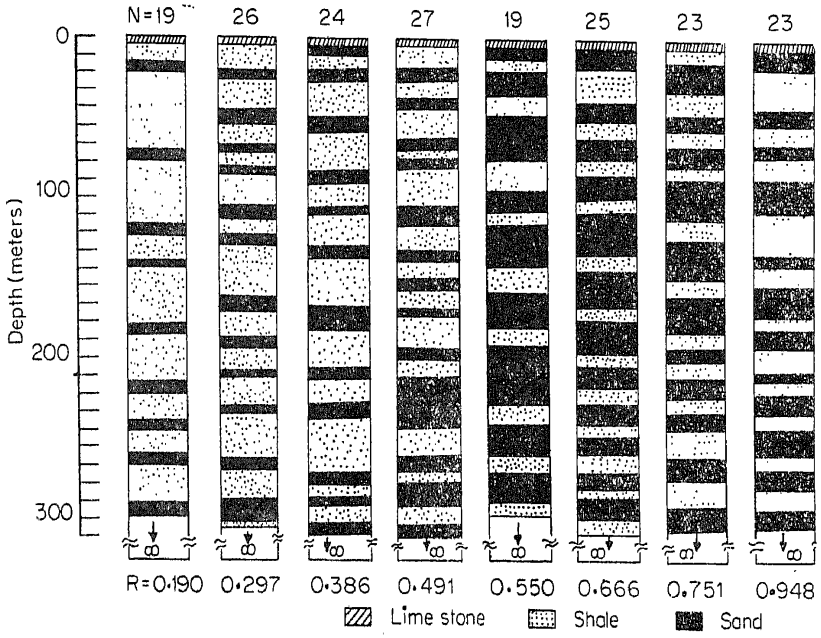

Figure 2. Lithological variations of some representative models. N = number of layers; Ra = Sandstone-shale ratio.

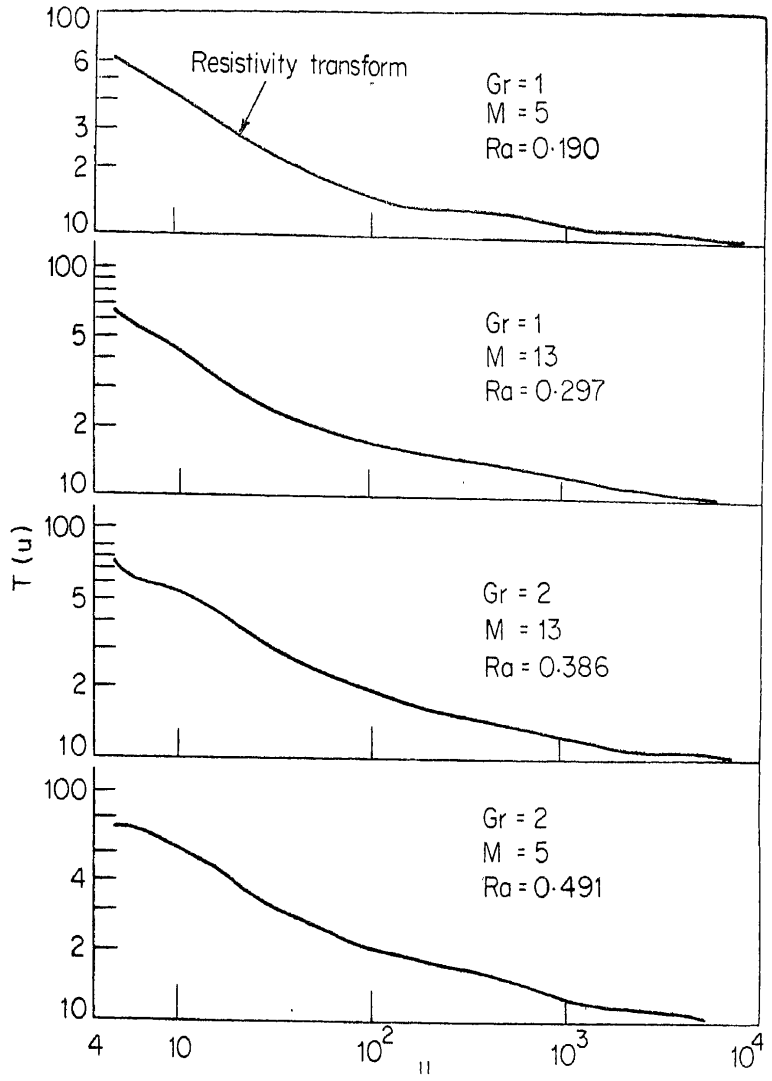

Figure 3. Resistivity transform functions. Gr = Group No.; M = Model No.; Ra = Ratio values.

of different curves for various sandstone-shale ratios over each other also did not bring out any appreciable difference amongst themselves.

4.3. *Amplitude spectrum*

Figure 6 shows the amplitude spectrum of the resistivity transforms of the two selected models. It can be observed that each curve is sharply decreasing till threshold frequency from where its assumes it shape in the form of the letter 'M'. It is a matter of speculation that the frequency (threshold) may change if the specifications on the layer parameters are changed. Further, it is found to be difficult to extract out any discriminating parameter from this as it exhibits very slight changes.

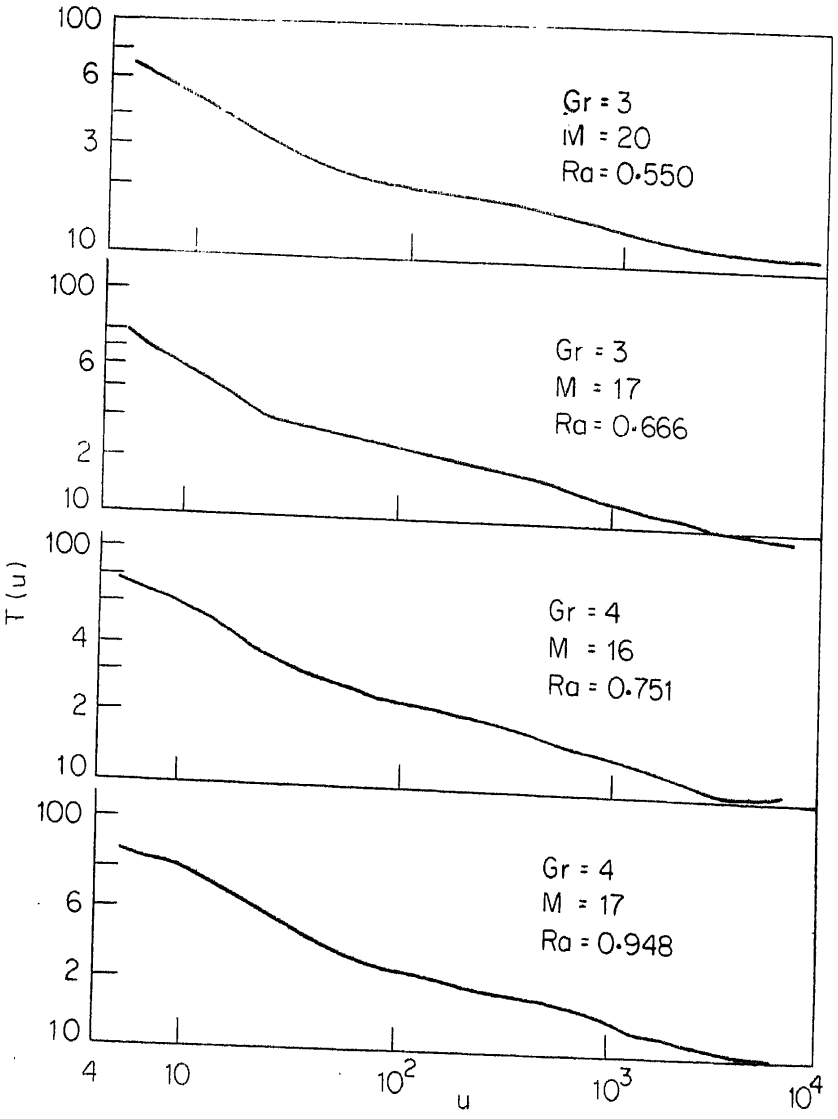

Figure 4. Resistivity transform functions of some representative models.

4.4. *Power spectrum*

Figures 7 to 10 show the power spectrum for representative models. Here also the descending nature of the spectra upto a threshold frequency can be observed from where it assumes a 'M' shape pattern. Detailed study of power spectrum revealed two characteristics that could serve as sandstone-shale discriminants, namely,

(i) the amplitude at the first significant minimum (P_1), and
(ii) the amplitude at the second significant minimum (P_2) at which minimum energy has built up.

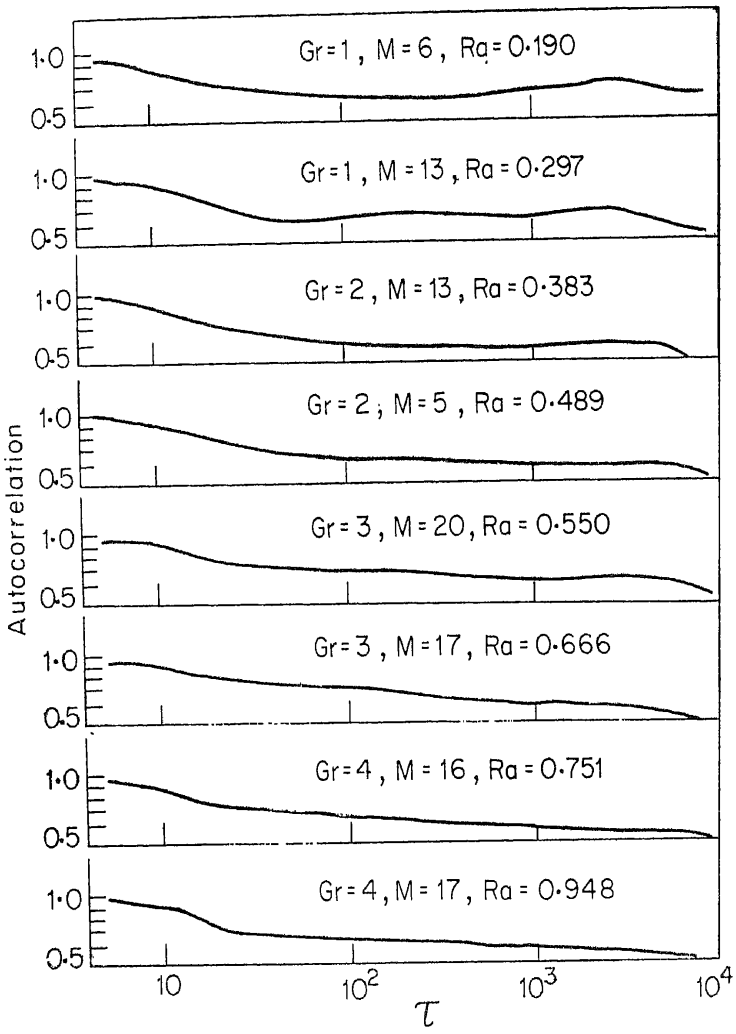

Figure 5. Autocorrelation functions of resistivity transforms of eight models.

P_1 and P_2 have been plotted against sandstone-shale ratios in figures 11 and 12. It can be observed that the general trend of these values are decreasing as sandstone-shale ratio values increase. The plot between the amplitude P_2 against sandstone-shale ratio (figure 12) shows that there are two clusters of points (1 and 2) separated by a clear-cut gap. The clusters show separate but more or less parallel inverse trends. It may be pertinent to mention that initially only 84 models were generated and their P_2 values were plotted against sandstone-shale ratios and the plot was of the nature discussed above, showing a gap between clusters 1 and 2. It was felt that the inadequacy of the number of models might have given rise to this gap. As such another set of 84 models with starting random number altogether different from the one chosen for generating first set of 84 models, were created and P_2 vs sandstone-shale plots were prepared. Significantly the new set of data gave exactly similar results, thereby signifying the

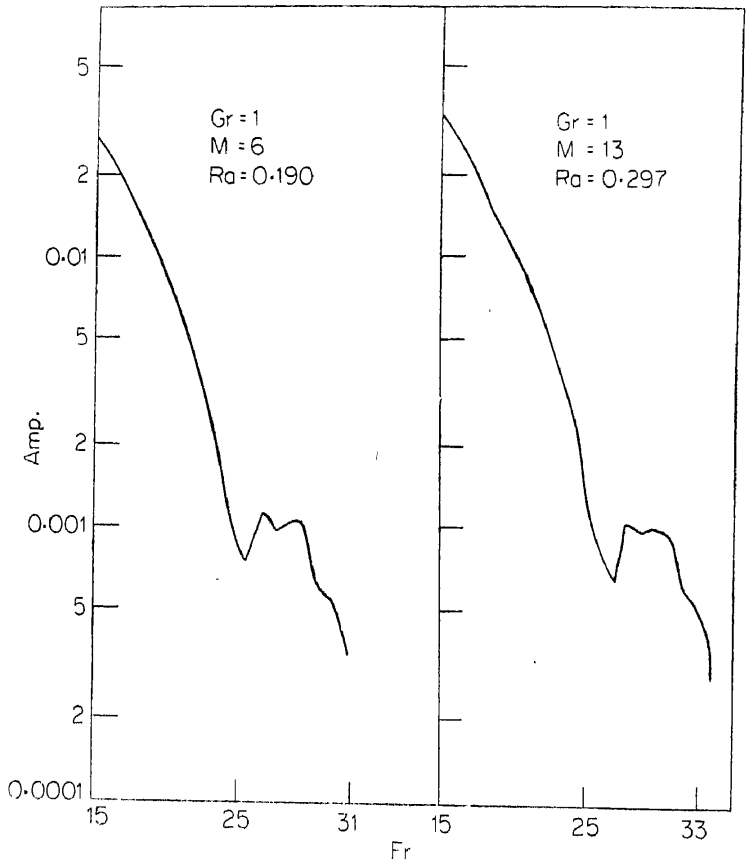

Figure 6. Amplitude spectrum of some representative models. Fr = frequency.

presence of the above-mentioned gap as an inherent and characteristic feature of this relationship. These cluster of points were subjected to correlation and regression analysis separately. The product moment correlation coefficients for clusters 1 and 2 are $-0{\cdot}9$ and $-0{\cdot}7$ respectively. Because of these high correlation coefficients, regressior lines of P_2 on sandstone-shale were fitted to these clusters (figure 12). The F test was applied to test the goodness of fit of the regression line. It was found that regression line fitted very well at 5% level of significance. Table 3 shows the test for these values. The test statistics for line 1 to apply F test are—degree of freedom $\nu_1 = 1$, $\nu_2 = 81$, critical region $F > 3{\cdot}60$ and for line 2—degree of freedom $\nu_1 = 1$, $\nu_2 = 79$, critical region $F > 3{\cdot}29$ (table 4). In both the cases, the computed F value falls well within the critical region, so we reject the hypothesis that the variance about the regression line is no different than the variance in the observations.

The goodness of fit of the line to the data point can be defined by

$$R_1^2 = SS_R/SS_T = 0{\cdot}799 = 79{\cdot}9\%,$$

$$R_2^2 = SS_R/SS_T = 0{\cdot}453 = 45{\cdot}3\%,$$

and the corresponding multiple correlation coefficients are $0{\cdot}894$ and $0{\cdot}673$.

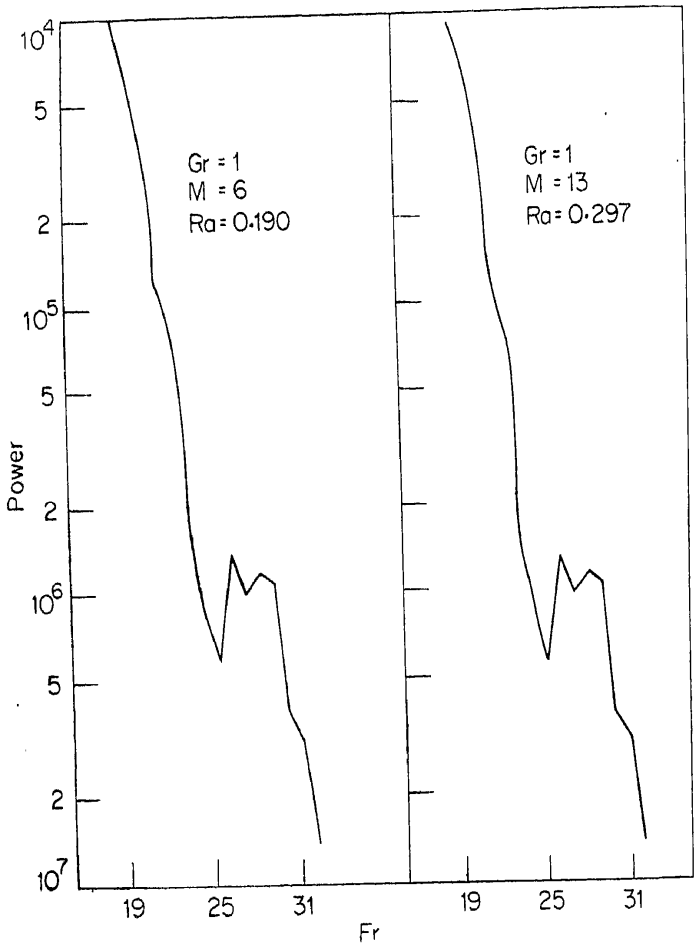

Figure 7. Power spectrum of some representative models.

Since the values of the goodness of fit are considerably high we feel that these lines may help estimate the sandstone-shale ratio from P_2. However, the relationship between P_2 and sandstone-shale ratio is very sensitive. A slight variation in the value of P_2 may give a large variation in the sandstone-shale ratio values.

4.5. *Log-spectrum and phase-spectrum*

The log-spectrum and phase-spectrum of all the models were studied but they do not hold promise in achieving any significant contribution for getting sandstone-shale ratio values.

5. Conclusions

The conclusions of this study are based on the following specifications;

(i) 168 models of sandstone-shale were generated in two stages, using Monte-Carlo simulation technique. The total thickness of these models has been

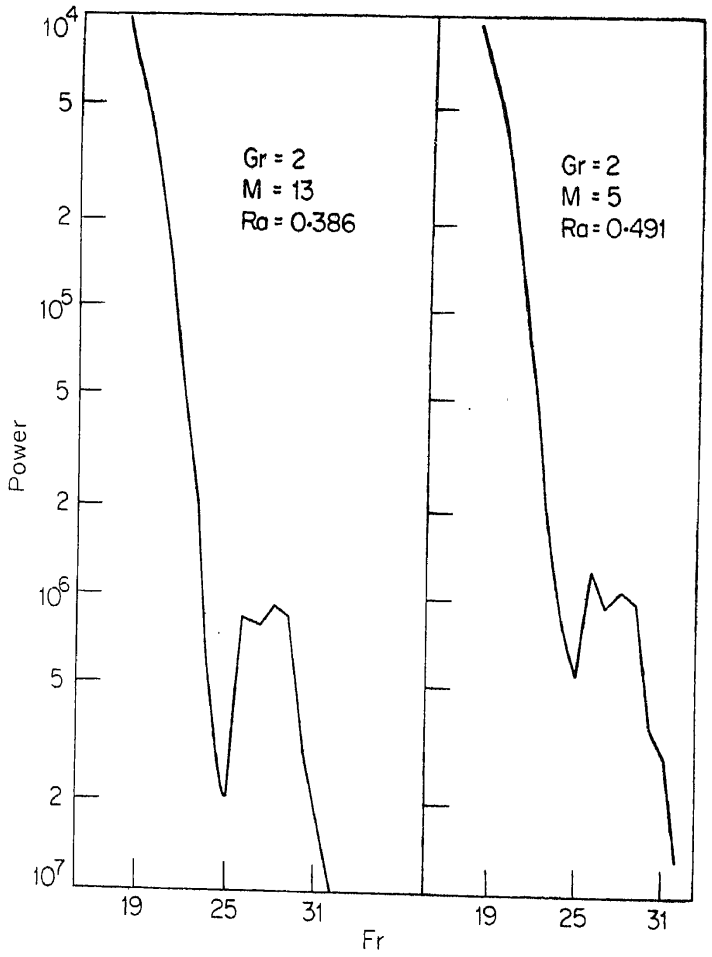

Figure 8. Power spectrum of some representative models.

kept at 300 m ± 3 m below a 5 m thick massive limestone bed which caps these sequences and is a surface layer.

(ii) These models have been assumed to be under artisan conditions.

(iii) The resistivities of shale, water-bearing sandstone and limestone capping the models have been realistically chosen as 10, 40 and 80 ohm m respectively.

The salient features of the present study are:—

(i) The resistivity transform function and autocorrelation function show a decreasing trend with increasing u and τ values whereas the amplitude, power and log spectra of the resistivity transform show initially a sharp inverse trend with frequency, till a threshold value around 25, after which it assumes the shape of the letter 'M'.

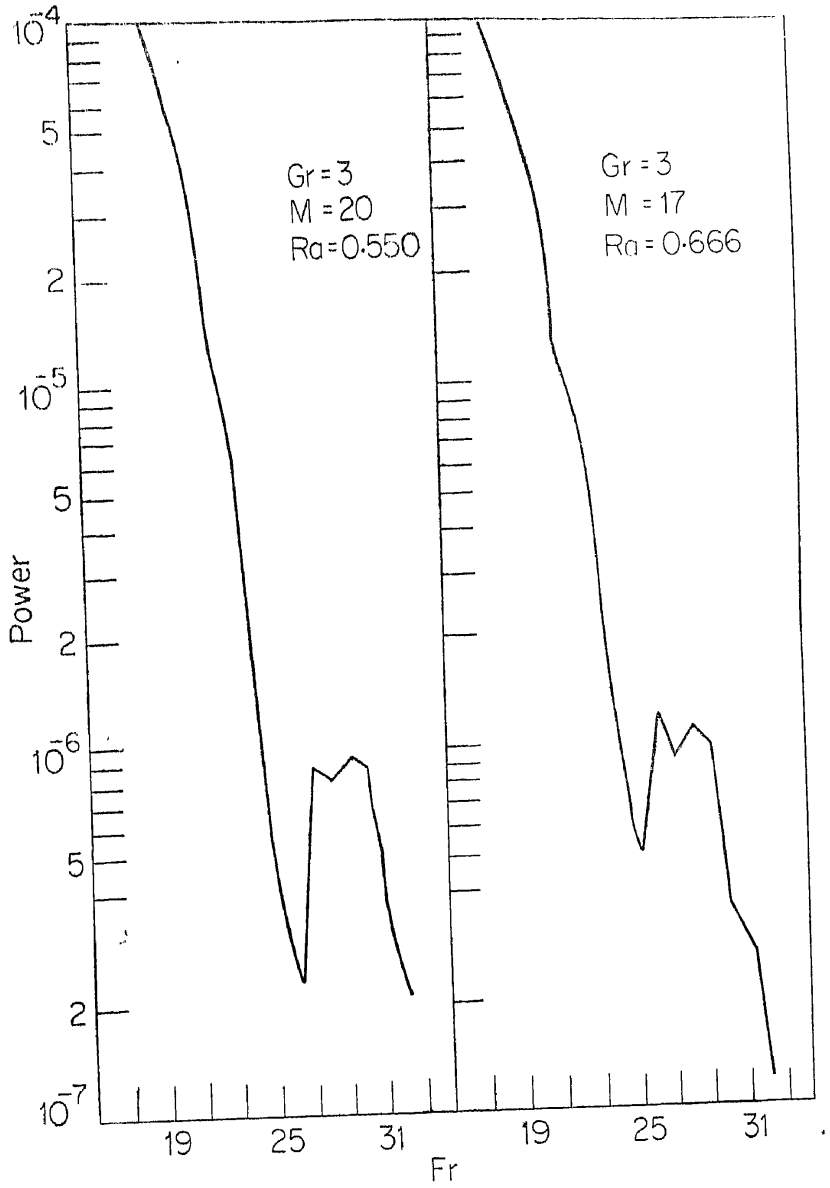

Figure 9. Power spectrum of some representative models.

(ii) Of all the parameters, power spectrum appears to be of importance. Its P_2 character shows a high negative correlation with sandstone-shale ratio. Two parallel inverse trends with a gap at P_2 value between 29 and 44, is an inherent and chcaracteristic feature of the relationship of P_2 and the sandstone-shale ratio. The reasons for the appearance of this gap is not clear at present. However, it is surmised that this linear relationship may help in estimating the sandstone-shale ratios in an area where the regional geology indicates the possibilities of the presence of subsurface sandstone shale sequence.

Table 3. Calculations for fitting linear regression lines.

	$\sum_{j=1}^{\eta_i} X_{i,j}$	$\sum_{j=1}^{\eta_i} Y_{i,j}$	$\sum_{j=1}^{\eta_i} X_{i,j}^2$	$\sum_{j=1}^{\eta_i} Y_{i,j}^2$	$\sum_{j=1}^{\eta_i} X_{i,j} Y_{i,j}$	$SD(X_i)$	$SD(Y_i)$	Cov (X_i, Y_i)	Regression Coefficient b_i of Y_i on X_i
For Regression Line 1 $i = 1$ $\eta_1 = 83$	43·855	4375·35	26·431	$23{\cdot}21 \times 10^6$	2249·391	1·805	34·435	−62·139	− 19·06
For Regression Line 2 $i = 2$ $\eta_2 = 81$	48·407	1704·13	32·520	$37{\cdot}64 \times 10^6$	964·058	1·895	42·280	−52·359	− 15·138

The equation of linear regression line 1 is $Y + 19{\cdot}063\,X = 62{\cdot}787$
and that of 2 is $Y + 15{\cdot}138\,X = 30{\cdot}083$.

Table 4. Completed ANOVA for significance of regression of parameter values of sandstone-shale values.

	Source of variation	Sum of squares	Degree of freedom	Mean square	F test computed	F tabulated
Line 1	Regression	$SS_R = 1180{\cdot}4725$	1	$MS_R = 1180{\cdot}4725$		
	Deviation	$SS_D = 297{\cdot}2875$	81	$MS_D = 3{\cdot}6702$	$\frac{MS_R}{MS_D} = 322{\cdot}173^+$	3·60
	Total	$SS_T = 1477{\cdot}760$	82			
Line 2	Regression	$SS_R = 810{\cdot}33$	1	$MS_R = 810{\cdot}33$		
	Deviation	$SS_D = 977{\cdot}265$	79	$MS_D = 12{\cdot}370$	$\frac{MS_R}{MS_D} = 65{\cdot}508^+$	3·29
	Total	$SS_T = 1787{\cdot}595$	80			

+ Significant at the 5% level of significance.

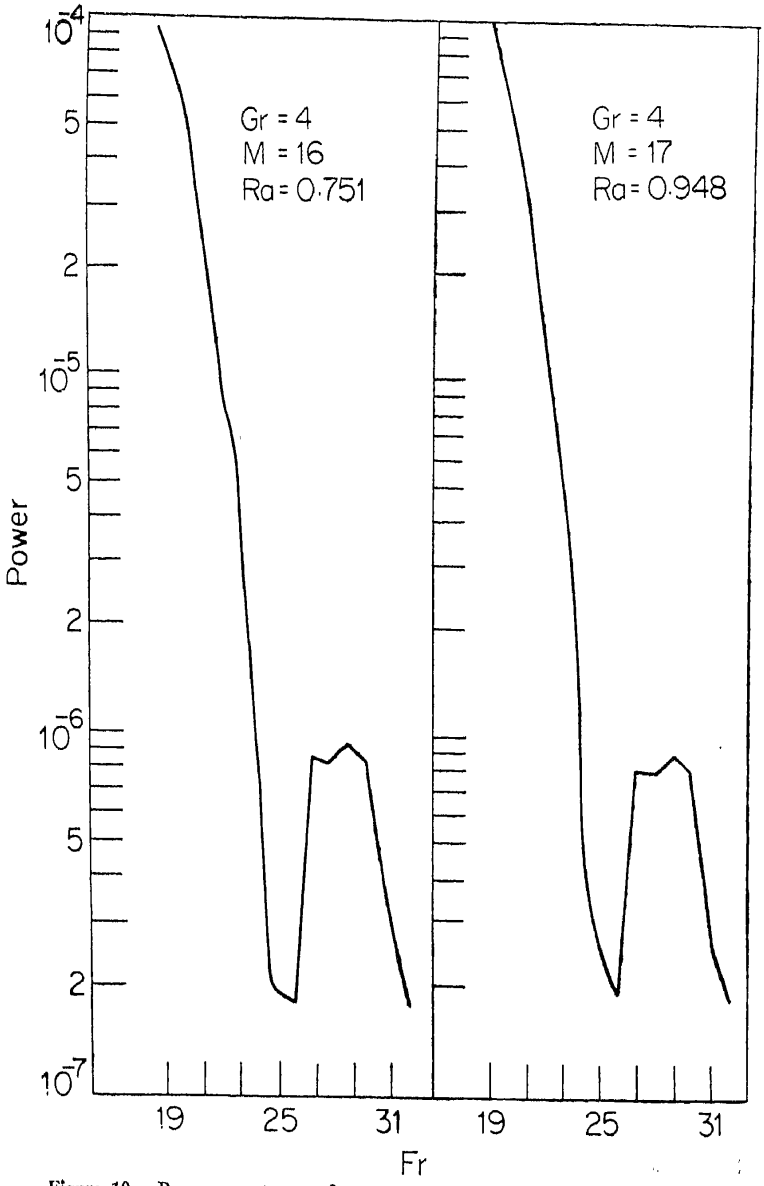

Figure 10. Power spectrum of some representative models.

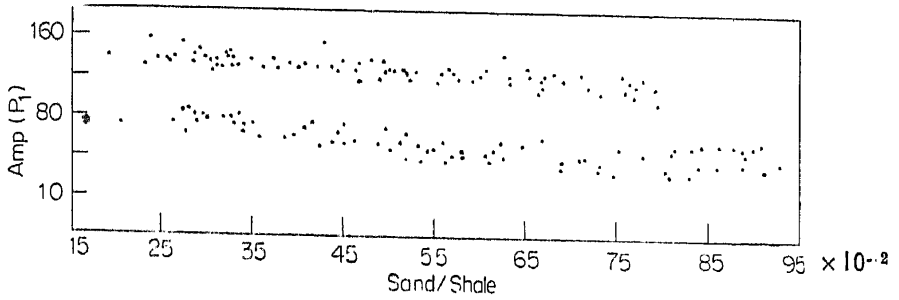

Figure 11. Plot of power amplitude (P_1) vs sandstone-shale ratio values.

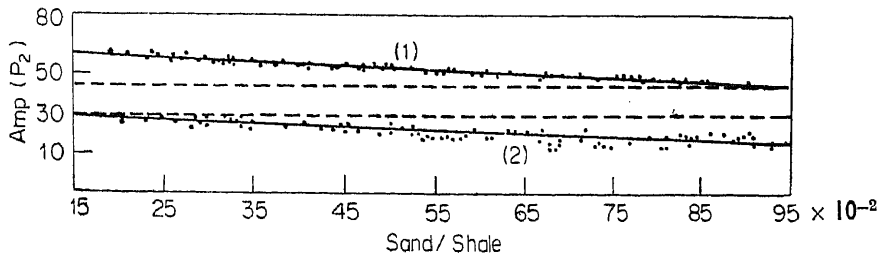

Figure 12. Plot of power amplitude (P_2) vs sandstone-shale ratio values.

References

Avasthi D N and Verma S K 1973 Presented at the Indo-Soviet symposium on Recent Trends in Exploration of Mine and Groundwater New Delhi

Flathe H 1955 *Geophys. Prosp.* **3** 268

Gardner G H F, Gardner L W and Gregory A W 1974 *Geophysics* **39** 770

Ghosh D P 1971 *Geophys. Prosp.* **1** 192

Harbaugh J W and Carter B G 1970 *Computer simulation in geology* (New York : John Wiley)

Khattri K N and Gir R 1975 *Oil Gas J.* **24** 89

Khattri K N and Gir R 1976 *Geophys. Prosp.* **24** 454

Khattri K N, Sinvhal A and Awasthi A K 1979 *Geophys. Prosp.* **27** 168

Koefoed O 1970 *Geophys. Prosp.* **16** 71

Mathieu P C and Rice G W 1969 *Geophysics* **34** 507

Savit C H and Matekar E J 1971 *Proc. 8th World Petroleum Conf.* (London : Appl. Science Publ.)

Smith M K 1969 Presented at the 54th Meeting of AAPG, Dalls

Sri Niwas, Pande K K, Gaur V K and Awasthi A K 1978 *Paper presented at the AEG Seminar on Exploration Geophysics*, Andhra University, Waltair

Stefanesco S S and Schlumberger 1930 *J. Phys. Radium* **7** 132

Taner M T and Koehler F 1969 *Geophysics* **34** 858

Taner M T, Cook E E and Neidell N 1970 *Geophysics* **35** 551